Annual Methodological Archive Research Review
http://amresearchreview.com/index.php/Journal/about
Volume 3, Issue 9 (2025)

Online ISSN 3007-3197
Print ISSN 3007-3189

http://amresearchreview.com/index.php/Journal/about

Ab Initio Computational Study of Intrinsic Half-Metallicity in Binary Alkali Metal Chalcogenides: KX (X = S, Te)

Dr. Fasih Udin (Corresponding Author)
Department of Physics, Grand Asian University, Sialkot, 7 km Pasrur Road, Sialkot, Punjab 51310, Pakistan Email: fasih.uddin@gaus.edu.pk

Dr. Amad Ud Din
Manager Training Program, Information Technology Services, Fatima Jinnah Women University, Rawalpindi, Pakistan

Dr. Asfand Yar
Qurtuba University of Science and Information Technology Dera Ismail Khan

Dr. Tanvir Ahmed
Department of Computer Science & Software Engineering, Grand Asian University, Sialkot, 7 km Pasrur Road, Sialkot, Punjab 51310, Pakistan.
Email: drtawaraich@gmail.com

ABSTRACT

The current article is based on first principle full-potential linearized augmented plane wave and density functional theory (DFT) that used to analyze KX (X=S and Te) potassium binary alkali–metal chalcogenides. It employed to determine the exchange-correlation energy and potential of various compounds like sodium chloride and caesium chloride in different crystalline phases utilizing the GGA and the modified Becke–Johnson method. Lattice parameters of KS and KTe are 8.586, 8.586, 5.921 and 5.659, 5.659, 12.448 respectively. The spin-polarized p orbital's lie in group VI elements of the periodic table containing half-metallic and half-magnetic DFT simulations were used to investigate chalcogenide materials due to their wide bandgaps and strong optical absorption intensities. The KS and KTe are excellent photovoltaic and infrared sensing materials. There are two distinct bandgaps in KS: 1.29 eV direct bandgap for KS and 1.47 eV direct bandgap for KTe. The bandgaps in both formations allow for the generation of solar power. The structures with both conduction and valence bands are controlled by chromium d orbitals and chalcogenide p orbitals stoichiometrically. While the KS bands are so small, the density of states above the conduction band is substantial. Above the conduction band, there are only 15 KTe3 states/eV. The improved values may affect the industrial impact and cost with the increase in corresponding values.

Key Words: First Principal Calculations, Density Functional Theory (DFT), Bandgap, Optical Absorption, Solar Energy Generation.

Annual Methodological Archive Research Review
http://amresearchreview.com/index.php/Journal/about
Volume 3, Issue 9 (2025)

Online ISSN 3007-3197
Print ISSN 3007-3189

http://amresearchreview.com/index.php/Journal/about

Introduction

Currently study analyze the physical properties of KX (X= S and Te) compounds in a Wurtzite structure at constant volume. The selected binaries are revealed to be roughly twice ferromagnets with a magnetic polarity of B per formula unit and split gaps of 0.24, 0.52, and 0.62 eV respectively [1]. These compounds' 1/2 can be sustained up to a lattice compress of 9 percent; The KX (X= S and Te) semiconductors that have been created artificially carrying great information to utilize in the creation of useful device applications [2].

The First-principles equation is used to assess the structural, electronic, and magnetic capabilities of KX (X=S, Se, and Te) dual alkali–metal chalcogenides compositions using the filled to the brim linearized y - polarized approach. Fock and mBJ-GGA-PBE were used to determine the conversation energy and potential of these components in diverse crystal phases, We determined that the uncharged Preliminary examinations phase has been the most stable phase for KX ideal material. Internal factors, bulk moduli, first-pressure gradients, and crystalline size all correlate well with the simulated result. The inclusion of roll p orbitals in the group's VI elements KX (X= S and Te) may be shown in the electronic structures and density of states.

Frequencies of KX (X= S and Te) alloys have been projected based on analyses of the elastic and electrochemical properties of the compositions [3]. Similarly, the layered chalcogenides can behave as charge transfer hosts because of the low chemical bonds or dipole - Dipole interactions that link the layer together. The intercalation of alkali metals, alkaline earth, rare earth, and organic groups or compounds can result in a wide range of novel compounds and fascinating physical and chemical characteristics when the spacer layers are placed into the structure. The selected compounds reveal some remarkable facial appearance in the electronics and structural properties and associated with the fermium partially filled f electron shells and interact powerfully with the lattice when delocalized. This shows that behavior of 4f electron of rare earth ion and also addition of neighboring ion f states into p states. The majority of both compounds go through at high pressure from the NaCl (B1) type to CsCl (B2) type the first order structural phase transition. Therefore, isolated because the structural properties are apprehensive, some pnictides of fermium group investigated by X-ray diffraction at high-pressure technique. As well as the experimental study, theoretical calculation base on DFT and is used to reproduce the experimental facts and to find fascinating properties in which experimental dimensions are to be done.

Methodology

We implemented density functional theory (DFT) as described in the Vienna Ab Initio Simulation Package (VASP) code, which combines the "projector-augmented wave (PAW)" and "KX (X= S and Te)" pseudopotentials and a commercial airliner basis set to increase the electromagnetic wave function. "PBE–GGA" (Pardew–Burke–Enercon) simulated the share implications. We used spin-polarized simulations in which the iron ions had different spin sequences imposed. On-site Photoelectric term (U = 4 eV) for the chromite ions and "KX (X= S and Te)" was included in the analysis, as is Hund's transfer term (J = 0.07eV). Experiments on crystallites were included in our estimates except for SiCrTe3, whose X-ray results from "Casto" and associates had been used for "KX (X= S and Te)". By this comparison, the energy

Annual Methodological Archive Research Review
http://amresearchreview.com/index.php/Journal/about
Volume 3, Issue 9 (2025)

Online ISSN 3007-3197
Print ISSN 3007-3189
http://amresearchreview.com/index.php/Journal/about

level was established.

The entire, linearized, augment plane wave (FP–LAPW) approach is being used to predict the electronic band architectures, frequency of components “KX (X= S and Te)”, and surface properties. The interspace between muffin tin spheres in each atom's center and the transitional area outside spheres is often to as the "interstitial space." An amplification in spheres harmonies up to is achievable for the electromagnetic plane wave when it is encapsulated within the spherical, where it is interpreted as an electron neutrino expression. The emission spectrum is developed into a waveguide in intermembrane space, with a total wave vector of Fixing, where is the circumference of the least sphere, specifies the maximum waveform vector “KX (X= S and Te)”. Using Wavelet transform, the electronic structure may be increased up to the Bulk counterpart. The identical U and J variables used in the “VASP” energy output analysis were used for on-site Strong interactions. Self-consistent field computations are carried out until the Ry and e's energy and charging are harmonized. Because the magnetism polarity in the nucleus was acquired from the “VASP” analysis, we utilized spin-polarized for our estimates.

The optical features of the chromium chalcogenides were found from the electromagnetic calculations. These inertia matrix elements were being used to generate the dielectric function's fictitious element.

$$\hat{H}1\Psi 1 = \widehat{E1}\Psi 1 \qquad (3.1)$$

There, p is the momentum operator, and f is the Fermi-Dirac distribution function with an average amplitude of. A transmittance was obtained by applying a Kramer–Kroni translation to get the system” of the complex permittivity:

$$\widehat{H1} = \hat{T}_e + \hat{T}_N + \hat{V}_{Ne} + \hat{V}_{ee} + \hat{V}_{NN} \qquad (3.2)$$

Density Functional Theory would be used for all physical, heat, and ionic conductivity calculations. Maximum potential better definition amplified plane wave plus local orbitals “KX (X= S and Te)” and “KX (X= S and Te)”, as described in the WIEN2k code, would be used for these simulations. Exact exchange effects were discussed using the basis set approximation parameterized by R. d., Burke, and Retinopathy (PBE).

$$\nabla^2_{q'} = \frac{\partial^2.}{\partial x^2_{q'}} + \frac{\partial^2.}{\partial y^2_{q'}} + \frac{\partial^2.}{\partial z^2_{q'}} \qquad (3.3)$$

In the chromium structure with the unit group F-43 m, “CdX” products crystallize The X atom set to and the Cd particle is set to" (0.25, 0.25, 0.25)". When it comes to reducing the energy produced, we used "Murnaghan's" equation of state. As a function “Kx (x= S and Te)”, the solution geometrical properties have been identified. To the relative success of the energy Matrix value, the simulations are performed with “Kx (x= S and Te)” = 9. “kmax” is the greatest wave vector value, whereas RMT is the maximum radius of the muffin tin (MT) hemispheres.

$$\hat{H}1 = \hat{T} + \hat{V}_{Ne} \qquad (3.4)$$

Calculations have been done employing "2.37, 1.73, 1.91, and 2.35"a.u. (atomic units) pastry radii (RMT) for "Cd, S, Se, and Te", respectfully. A frequency of 14.0 Bohr-1 was used for the utmost “Gmax”. The tangential velocity lmax of the subatomic microspheres has been enlarged to a highest value of 10." Brillouin zone (BZ)"in metal structure has been compressed to a matrix of " KX (X= S and Te)".

Annual Methodological Archive Research Review
http://amresearchreview.com/index.php/Journal/about
Volume 3, Issue 9 (2025)

Online ISSN 3007-3197
Print ISSN 3007-3189
http://amresearchreview.com/index.php/Journal/about

$$\hat{H}1 \quad \Psi 1 \quad = E1 \quad \Psi 1 \qquad (3.5)$$

$$E_{tot} = E1 \quad + E1 \qquad (3.6)$$

A sum of "0.0001Ry and 0.001e", respectfully, have now been obtained in the iterations. The ternary metal oxides zeolites of the type, where X is S, Se, or Te, are also an integral piece. Magnetic effects are prominent in this material owing to the presence of chromium, and this has now spurred new interest in them. They contain "SbCrSe3", “Kx (x= S and Te)” which has also been studied as a magnetic particle with ferrous or highly conductive features, and "SiCrTe3.

$$|\Psi(\mathbf{x}_1, \mathbf{x}_2, \dots, \mathbf{x}_N)|^2 \, d\mathbf{x}_1 \, d\mathbf{x}_2 \dots d\mathbf{x}_N \qquad (3.7)$$

Those although their preparation has been recorded for ages, most of these elements, especially numerous lanthanide chromium sulphones, have not been properly explored. For several chromium chalcogenides, we give first-principles estimates based on evolutionary psychological crystals data, but even though the electronic field magnetic characteristics have not been completely studied.

$$\Psi(\mathbf{x}_1, \mathbf{x}_2, \dots \dots, \mathbf{x}_N) = -\Psi(\mathbf{x}_1, \mathbf{x}_2, \dots, \mathbf{x}_N) \qquad (3.8)$$

Total energy calculations let us estimate the magnetic ordering at 0 K and then compute the optical characteristics of the material to assess its utility in various applications. Only "PCrSe3, SiCrTe3", “KX (X= S and Te)” and the "NH4CdCl3" prototype crystals, all of which are in spatial group 62, were not included in the study. It has seven coordinating in between a site and indeed the chalcogen atom "(X = S, Se, or Te)" in this shape. The complexes in this configuration share borders instead of crossing sides like in the perovskite materials.

$$\int \dots \int |\Psi(\mathbf{x}_1, \mathbf{x}_2, \dots, \mathbf{x}_N)|^2 \, d\mathbf{x}_1 \, d\mathbf{x}_2 \dots d\mathbf{x}_N = 1 \qquad (3.9)$$

First-principles " KX (Se and Te)" binary kcl change significantly are studied geometrically, technologically, and magnetized using a full-potential rollex11 augmenting plane wave methodology density functional theory “(DFT. NaCl (B1), CSci (B2), ZB (B3), and Nia’s (B8)" are crystals from distinct crystallization phases. Simulations of the transfer energy and potentially were carried out using the gga approximate "(GGA-PBE)" as well as the refined Finished with a herringbone technique "(mBJ-GGA-PBE)".

$$\hat{H}1 = -\sqrt{\frac{1}{4}\sum_p \nabla^2 \vec{r}_p} + \sqrt{\frac{1}{4}\sum_{p \neq q} \frac{1}{|\vec{r_p} - \vec{r_q}|}} + \sum_{p,q} \frac{Z_p}{|\vec{R_p} - \vec{r_q}|}$$

$$= \hat{T}_n + \hat{V}_{ee} + \hat{V}_{ext} \qquad (3.10)$$

KX binary compounds are most robust in the Higher quality phase, which is nonmagnetic. There is a clear agreement between its computed lattice constant, bulk young ’s modulus, corresponding first-pressure derivatives markets, and other simulated data. Tilt "[Formula: see text]" orbitals in the group VI elements are important for the semi and half-magnetic characteristics of the electronic structures and carrier density. Apart from "KSe and KTe in the CSci and Nia’s" phases, all "KX ([Formula: see text], Se and Te)" compounds have integer ferromagnetism of 1"[Formula: see text]" in all phases. the HM divides "[Formula: see text] for each formula unit)". "KX (X= S and Te)” has the greatest numerical value, indicating that it is much more cationic in nature. Measuring physical behavior with Deformation Between "0.39 and 0.41, the compaction of "CdX" compounds reveals that all of them

Annual Methodological Archive Research Review
http://amresearchreview.com/index.php/Journal/about
Volume 3, Issue 9 (2025)

Online ISSN 3007-3197
Print ISSN 3007-3189
http://amresearchreview.com/index.php/Journal/about

are compressed.

$\Psi_H(r) = \phi(r_1)\,\phi(r_2)\,\ldots..\phi(r_N)$ (3.11)

The methodology of the study is to study "Ab Initio of intrinsic Half Metallicity" in combination with alkali metals. To study the intrinsic half metallicity in KX (X= S and Te). "To investigate, density functional theory (DFT) is used to demonstrate the properties of KX (X= S, and Te)". KX ideal material. Internal factors, bulk moduli, first-pressure gradients, and crystalline size all correlate well with the simulated result. The inclusion of roll p orbitals in the group's VI elements KX (X= S and Te) may be shown in the electronic structures and density of states.

$$\left[-\frac{h^2}{2m}\nabla^2 + V\right]\Psi(r_1, r_2 \ldots r_N) = E\Psi(r_1, r_2 \ldots r_N) \quad (3.12)$$

Except for "KSe" and "KTe" in the "CsCl" and "NiAs" phases, all KX (X=S, Se, and Te) composites show HM feature, with an integer field strength of 1B per compound and HM spaces. This is accurate in all processes. They have PF values of 2.3 W/cm K2 and 0.83 W/m K2 at ° c, accordingly.

$\phi(r_1)\,\phi(r_2)\,\phi(r_3)\ldots\phi(r_N) = \phi(r_3)\,\phi(r_2)\,\phi(r_1)\ldots\phi(r_N)$ (3.13)

There is little doubt that thermoelectric and spintronics can benefit from the small wide bandgap, spin-polarized, and high PF ratios also under study. It has now been found in the combinations KBr "NaBr" and KX- KX (X= S and Te), but experimental evidence indicates that only crystalline regular components should be formed in KX (X= S and Te) In furthermore, new stable and metastable phases within those molecules are projected.

$$\phi(r_1)\,\phi(r_2)\ldots\phi(r_N) \neq 0 \quad (3.14)$$

$$\Psi 1 = \begin{vmatrix} \psi_1 X_1 & \psi_1 X_2 \ldots & \psi_1 X_N \\ \psi_2 X_1 & \psi_2 X_2 \ldots & \psi_2 X_N \\ \psi_N X_1 & \psi_N X_2 \ldots & \psi_N X_N \end{vmatrix} \quad (3.15)$$

Where X written in the parenthesis represents coordinates of spin and also the space, this simple data used to calculate wave function covers much of the information need for the correct solution of Hamiltonian.

The point of more interest is that the wave function is anti-symmetric whenever the position of any two electrons is changed with each other. This characteristic is needed by Pauli Exclusion Principle, i.e.

$\Psi 1(X_1, X_2, \ldots\ldots, X_N) = -\Psi 1(X_1, X_2, \ldots\ldots, X_N)$ (3.16)

This wave function can be used to solve Hamiltonian in equations and compute total energy. Consider being an orthonormal set because we know that the value of the determinant remains the same when any two lines transformations are swapped. To show normalized, we use a Lagrange multiplier and set it to the lowest value.

$$\frac{\delta}{\delta\psi}\left[< H1 > -\sum_j \varepsilon_j \int |\psi_j|^2 dr = 0\right] \quad (3.17)$$

Now it reduces to equation called as one-electron equation given below,

$-\frac{1}{2}\nabla^2\psi_i(r) + V1\ \ (r)\psi_r + U(r)\psi_i(r) = \varepsilon_i\psi_i(r)$ (3.18)

Non-local potential is denoted by U(r) and V_{ion} represents potential which termsas local potential. This one-electron equation looks alike Schrodinger equations of single particle. The Hartree Fock equations are given by:

$$\varepsilon_i\psi_i(r) = \left(-\frac{1}{2}\nabla^2 + V_{ion}(r)\right)\psi_i(r) + \sum_j \int dr' \frac{|\psi_j(r')|^2}{|r-r'|}\psi_i(r)-$$

Annual Methodological Archive Research Review
http://amresearchreview.com/index.php/Journal/about
Volume 3, Issue 9 (2025)

Online ISSN 3007-3197
Print ISSN 3007-3189
http://amresearchreview.com/index.php/Journal/about

$$\sum_j \delta_{\sigma_i\sigma_j} \int dr' \frac{\psi_j(r')\psi_i(r')}{|r-r'|}\psi_j(r'.) \qquad (3.19.)$$

There are four terms on the right-hand side of the equation above.1st and 2nd terms in the right-hand side represent kinetic energy involvement and potential between electrons and ions. Furthermore, the third term, which we refer to as the Hartree terms, is just the electrostatic potential generated by N electrons' charge distribution.

$$E1[\rho(\mathbf{r})] = \int V_{ext}(\mathbf{r})\rho(\mathbf{r})\,d\mathbf{r} + F[\rho(\mathbf{r})] \qquad (3.20)$$

In above equation, the external potential describes electron Coulomb interactions with the nucleus. The electron density functional F [(r)], which is made up of kinetic energy T [(r)] and the inter-electronic potential Vee [(r)], is unknown but universal. A non-communicating system's specific kinetic energy can be calculated using the following formula as proposed by Kohn and Sham.

$$T_S = -\frac{1}{2}\sum_i^N(\varphi_i|\nabla^2|\varphi_i) \qquad (3.21)$$

Interacting and non-interacting systems have different kinetic energies. As a result, Kohn and Sham devised the following F [(r)] separation:

$$F[\rho(.\mathbf{r})] = T_S[.\rho(\mathbf{r})] + J[.\rho(\mathbf{r})] + E_{xc}[.\rho(\mathbf{r})] \qquad (3.22)$$

WhereE_{xc} stands for exchange-correlation energy, which is defined as

$$E1\ \ [\rho] = (T[\rho] - T_S[\rho]) + (E_{ee}[\rho] - J[\rho]) = T_C[\rho] + E_{nucl}[\rho] \qquad (3.23)$$

E_{xc}, the exchange-correlation functional, is like a scrap yard because it contains all of the unknowns. The final difficulty is how to define V_S so that the Slater determinant has a density that is similar to that of the real system. It makes it easier to write down the energy of a real-world, interconnected system:

$$E1[\rho(\mathbf{r})] = T_S[\rho] + J[\rho] + E1\ \ [\rho] + E_{Ne}[\rho]$$

$$= T_S[\rho] + \frac{1}{2}\int\int\frac{\rho(\mathbf{r_1})\rho(\mathbf{r_2})}{\mathbf{r_{12}}}d\mathbf{r_1}\,d\mathbf{r_2} + E_{xc}[\rho] + \int V_{Ne}\,\rho(\mathbf{r})\,d\mathbf{r} = -\sqrt{\frac{1}{4}\sum_{i.}^{N.}\langle\varphi_i|\nabla^2.|\varphi_i\rangle} +$$

$$\sqrt{\frac{1}{4}\sum_{i.}^{N}\sum_{j.}^{N.}\int\int|\varphi_i(\mathbf{r}_1.)|^2\frac{1}{\mathbf{r}_{12.}}|\varphi_{i.}(\mathbf{r}_2)|^2\,d\mathbf{r}_1\,d\mathbf{r}_2} + [\rho(\mathbf{r})] - \sum_{i.}^{N}\int\sum_A^M\frac{Z_A}{\mathbf{r}_{1A}}|\varphi_i(\mathbf{r}_{1.})|^2\,d\mathbf{r}_{1.}.$$

(.3.24)

E_{xc} is unknown in Equation (3.24). Finally, the circumstances under which the orbitals $\varphi_i$minimise the energy expression under the restriction $<\varphi_i|\varphi_j> = \delta_{ij}$ must be determined. As a result, the equation emerges given in Reference

$$\left[-\frac{1}{2}\nabla^2 + V_{eff}\mathbf{r}_1\right]\varphi_j = \varepsilon_i\varphi_i(3.25)$$

Results and Discussions

By computing the compounds of the complex impedance for infinitesimal stains, it has been found the constitutive equations of square "KX (X= S and Te)" compound having Crystalline structure. Strict straining "(-0.02-0.02)" has been made up as a way to avoid the production of primitive lattice carriers. The findings are in accordance with the measured result of "5.830, 6.084, and 6.480", respectively, with a maximum deviation of "3.63 percent. A concise overview of the microstructures is essential to carry out further research into its high electrical attributes. Framework developed and included into "KX (X= S and Te)" code component was used to evaluate the elastic moduli of "KX (X= S and Te)" compounds with cubic symmetry. With each of the

Annual Methodological Archive Research Review
http://amresearchreview.com/index.php/Journal/about
Volume 3, Issue 9 (2025)

Online ISSN 3007-3197
Print ISSN 3007-3189

http://amresearchreview.com/index.php/Journal/about

three elastic moduli, the necessary crystallographic aberrations are given in a cubic lattice. The predicted mechanical properties values are the valid contract between our projected and practically set point for the crystalline properties. Metallic bonding may occur while positive variation pressure builds. Due to positive Cauchy pressure and the metallic quality in their bonds, all "KX" compounds are stretchy. There is a significant connection between the "KS" and "KTe".[4] It has a considerable standard of ionic bonds (ductility) as compared to other molecules because of the catch pressure. The corresponding values of Young's modulus (Y) Stiffer materials have excellent values of Y, which denotes their degree of firmness. Stiffer metals also have cross-links. In relation to other "KX" substances, KX (x= S and Te) has the greatest numerical value, indicating that it is much more cationic in nature. Measuring physical behavior with deformation between "0.39 and 0.41, the compaction of KX compounds reveals that all of them are compressed Solids with critical piece have ratios between 0.25 and 0.5. We recognize that the KX compounds' interfacial tensions are fundamental since are about 0.4[5] in our scenario. Findings of this study, the theoretical results are verified to the structural features. Most of such materials, including KS, and KTe, have directional order at relatively low temperature but are ferromagnetic materials at air temperature, thus according to observations. According to scientific investigations, ferromagnetic compositions of KS and KTe are consistent with the theory prediction.[4] A l.52 or weak magnetoelectric is uncertain in the KS and KTe structures, and this is shown in our studies by the pretty small energy differential between spinning states and subtle difference.

Structural properties of KX (X = S)

Utilizing the empirical Birch-equation Murnaghan's of state, the equilibrium lattice parameters of both the fermium monopnictides KX (X = S) have also been optimized by lowering the crystal's overall energy (EOS). The simulations have been completed through the energy of KX (X = S & TE) and KX (X = S & Te) unit cell is a piece of NaCl and CsCl like shaped. It is obvious from the past work that both the nearby thickness measure (LDA) and GGA misinterpret the cross-section limits. [6]

In fundamental properties, cross-sections are consistent, least energy, least volume, and mass modulus, and they're ot altogether permanently established by utilizing the FP-LAPW approach with summed up point evaluation (GGA). The concluded cross fragment consistent for NaCl for KX (X = S & TE) 5.571å concurs well with primer worth of 6.163 Å. [7]

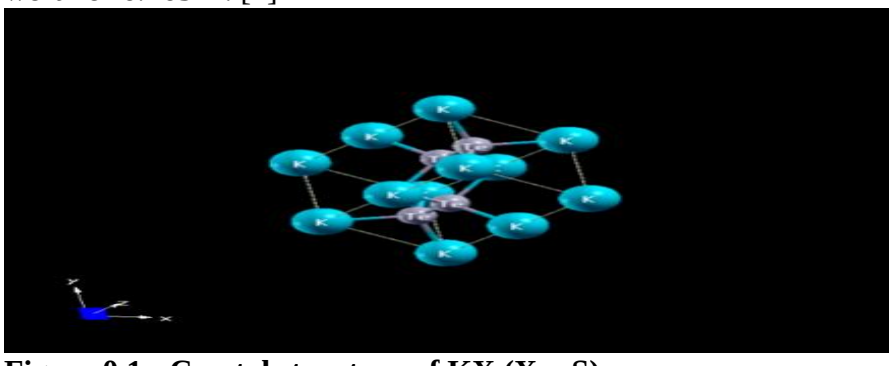

Figure 0.1 : Crystal structure of KX (X = S)

Annual Methodological Archive Research Review
http://amresearchreview.com/index.php/Journal/about
Volume 3, Issue 9 (2025)

Online ISSN 3007-3197
Print ISSN 3007-3189

http://amresearchreview.com/index.php/Journal/about

The Calculating experimentally determined parameters of KXX compounds in the B1 structure KX (0, 0, 0), and X (0.5, 0.5, 0.5) under the space group Pm3m (no. 221). B1 (NaCl-type) phase with KX (X = S & TE) compounds is energetically more favorable. For each type-structure of KX (X = S) compounds, the computed lattice constant (a0), bulk modulus (B0), first pressures derivative of the bulk modulus (B′), and lowest energy (E0) are presented. The magnetic phase endurance among these two KXX superior properties should also be known. The (E-V) curves showing the total energy of KX (X = S) materials as a consequence of various lattice constants in the B1 structural categories.

Structural properties of KX (X = Te)

In underlying properties, cross-section steady, least energy, least volume, mass modulus, and subordinates are determined by utilizing the FP-LAPW strategy with summed up inclination estimation (GGA). The concluded cross fragment consistent for CsCl for KX (X = S & Te) 5.576å concurs well with primer worth of 6.409Å. The Calculating experimentally determined parameters of KXX compounds in the B2 structure (KX (0, 0, 0), and X (0.25, 0.25, 0.25) under the space group F43m, are displayed for the first time by the GGA calculations (no. 216). The (E-V) curves showing the total energy of KX (X = S & Te) materials as a consequence of various lattice constants B2 structural categories. The figures show that the stabilization energy level of KX (X = Te) compounds is found in the B2 (CsCl-type) phase.

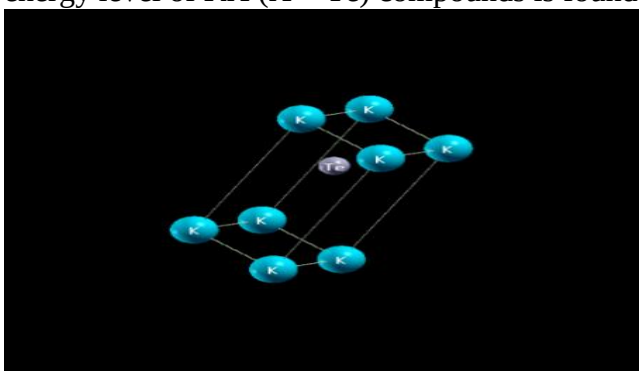

Figure 0.2 : Crystal Structure of KX (X=Te)

The magnetic phase endurance among these two KXX superior properties should also be known. The (E-V) curves of the entire NM phase, KX phase, including AKX phase have been completed in their important because it strengthens state to establish the stable magnetic condition in accordance with Birch-equation Murnaghan's of state (EOS), there they are shown for KX (X = Te). Results indicate that all KXX compounds have a stable magnetic framework for understanding as the NM state, which explains why these compounds behave in an NM manner. These data could be used as a reference for upcoming experimental investigations because there is currently no research or theoretical available data for the substances here investigated that can be compared with our findings.

X-Ray spectra of KX (X = S)

The structural phase shift of KX (X = S & TE) and KX (X = S & Te) to B1 to B2 at the highly pressurized range is investigated by X-ray diffraction. The research by

Annual Methodological Archive Research Review
http://amresearchreview.com/index.php/Journal/about
Volume 3, Issue 9 (2025)

Online ISSN 3007-3197
Print ISSN 3007-3189
http://amresearchreview.com/index.php/Journal/about

which focuses just on f and d electrons in atomic compounds, demonstrates that 5f - localized states dominate the studied spectra. Theoretical and experimental reviews of the optoelectronic characteristics of rare earth metal monopnictides have been done.

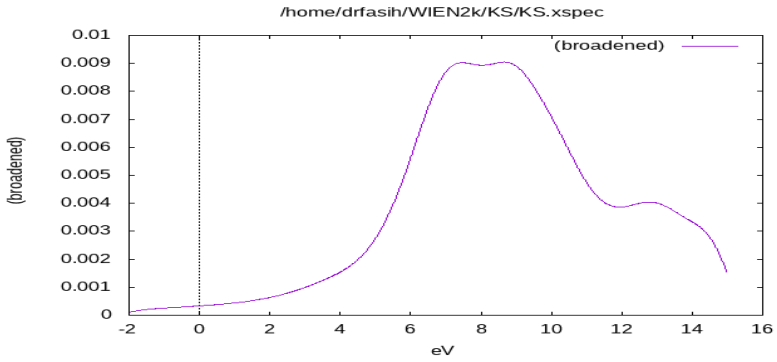

Figure 0.3: X-Ray Spectra Graph KX (X = S)

Numerous rare-earth monopnictides' electrical and magnetic properties have been studied, which came to the conclusion that the direct f-f interaction between nearby rare-earth atoms is often thought to be close to insignificant. A positive intensity X-ray diffraction method has been used to look at the crystal structure characteristics of RE-pnictides. Besides experiments, theoretical studies based on have also effectively confirmed experimental findings and are helpful in predicting intriguing features that have not yet been thoroughly investigated experimentally.

Band Gap of KX (X = S)

The GGA+U electronic properties structure of the twin fermium monopnictides KX (X = S & Te)) have been predicted using the FP-L/APW+lo technique and their dispersions, respectively, depending on the equilibrium structural properties. With regard to the KX (X = S & TE) compounds, the band structures are evidently maintained and along equally spaced orientations of the initial Brillouin zone of type B1.[8] It showed that the electrical bands overlap the region around the EF, proving that these compounds are metallic. The equilibrium lattice parameters were used to determine the spin-polarized band of the steady magneto structural state of the KX1xVxP alloys with their pure KX (X = S) compound. The energy of formation (Ef) is a crucial parameter to verify the researched KX compounds [9] permissible stability at absolute zero, where the lower the Ef value, the more stable the molecule is bonding between the atoms, which is advantageous since it promotes stability. All compounds' ability to maintain thermodynamic stability is confirmed by the computed values of all preceding energies being reported in the negative value of Ef for all the compounds.[10]

Annual Methodological Archive Research Review
http://amresearchreview.com/index.php/Journal/about
Volume 3, Issue 9 (2025)

Online ISSN 3007-3197
Print ISSN 3007-3189

http://amresearchreview.com/index.php/Journal/about

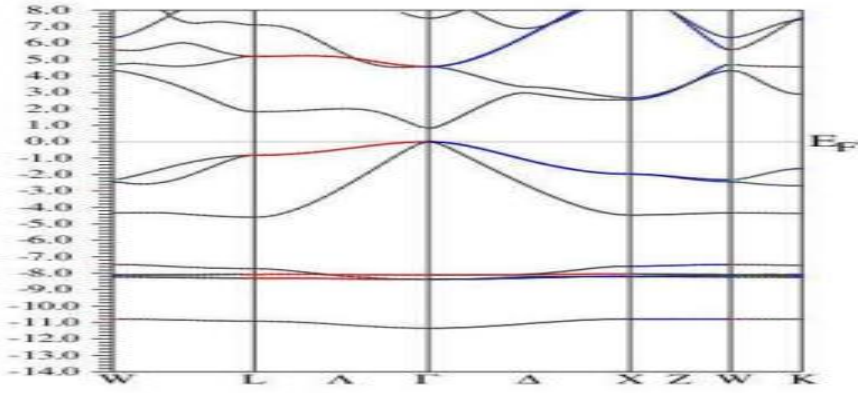

Figure 0.4 : Fermi energy of KX (X=S)

In order to predict the values of the structural energies parameterization for the alloys KX 0.75V0.25P, KX0.50V0.50P, and VP, and KX0.25V0.75P, respectively, the PBE-GGA is utilized.

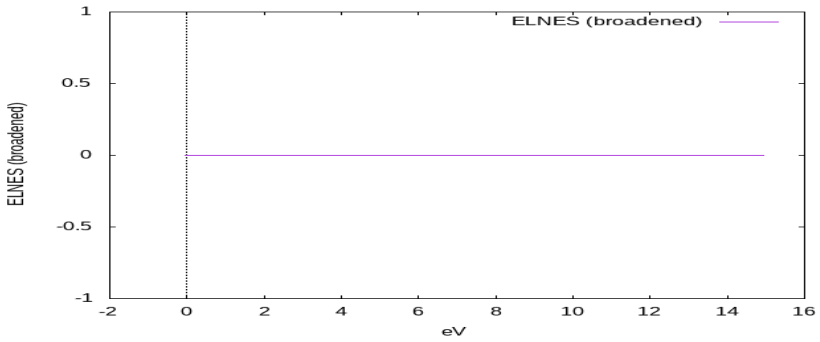

Figure 0.5 : Band Gap of KX (X =S)

Actually, the Brillouin region's first high symmetry directions dispersion relation instances are realized by the band structure. These results show that KX0.25V0.75P, VP, and KX0.50V0.50P due to the overlap of the bands of valence and conduction in the largest group (spin-up) and tiny fringe (rotation) conditions. Metal makes up the entirety of alloys.

Band Gap of KX (X=Te)

The self-reliable scalar relativistic is the band structures much the same way as the thickness of states for the B2 stage along the assorted value line's inside the GGA plot are given for KX (X = Te). Band structures are connected to the TDOS as well. Another metallic behavior is shown in the TDOS intensities of the two KX (X = S & Te) compounds, with the crowded region located in the higher and lower Fermi level. When KX 0.75V0.25P spins down, the conduction band's symmetry point, the bottom of the alloy, and the top of the valence band are all where this electronic structure contributes.

Annual Methodological Archive Research Review
http://amresearchreview.com/index.php/Journal/about
Volume 3, Issue 9 (2025)

Online ISSN 3007-3197
Print ISSN 3007-3189

http://amresearchreview.com/index.php/Journal/about

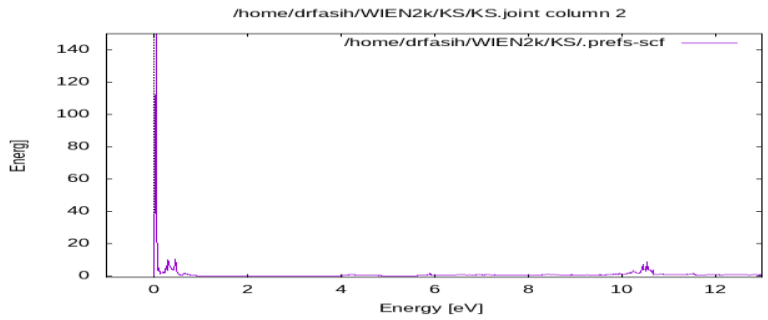

Figure 0.6: Band gaps of KX(X=Te)

Electron density

The price density distribution of positive atoms is used to explain the bonding function of the material. Covalent bonding is defined as the sharing of costs between the cation and anion, whereas ionic bonding is defined as the transfer of charge between them. The above structure arises mainly from the only available photoemission data by which is in good agreement with our calculated total density of states. It shown in figure with the help of scale ∇ (n) 0.0013, 0.0610, 0.1208, 0.1805, 0.2403 and 0.3000 and observed photoemission data.

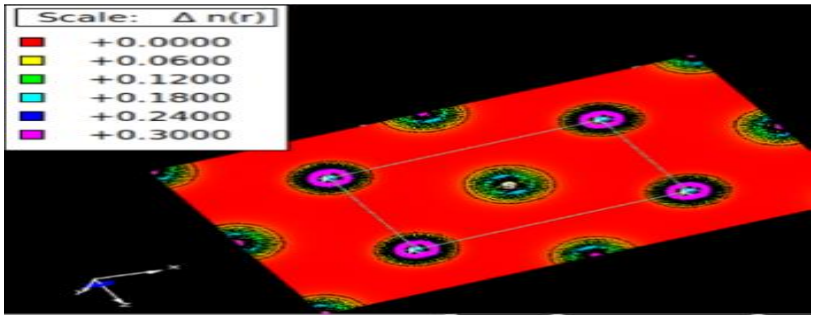

Figure 0.7 : Electron densities of KX (X = S)

Density of state KX (X = S)

The density of states can also investigate band shape (DOS). We concluded the aggregate and fragmentary densities of conditions for the KX (X = S) compound in the NaCl (B1) stage. The plots plainly show that the valence band (VB) shifts toward the Fermi degree with the anion. This band is overwhelmed by KX and X = S and Te states near the Fermi level. Over the Fermi degree, there is a blend of s, p, and f states. I have drawn the graph of the density of the states with the help of Wien2k software. Graphs are plotted between energy and DOS. Graph show increase and decrease in the intensity and DOS.

Annual Methodological Archive Research Review
http://amresearchreview.com/index.php/Journal/about
Volume 3, Issue 9 (2025)

Online ISSN 3007-3197
Print ISSN 3007-3189
http://amresearchreview.com/index.php/Journal/about

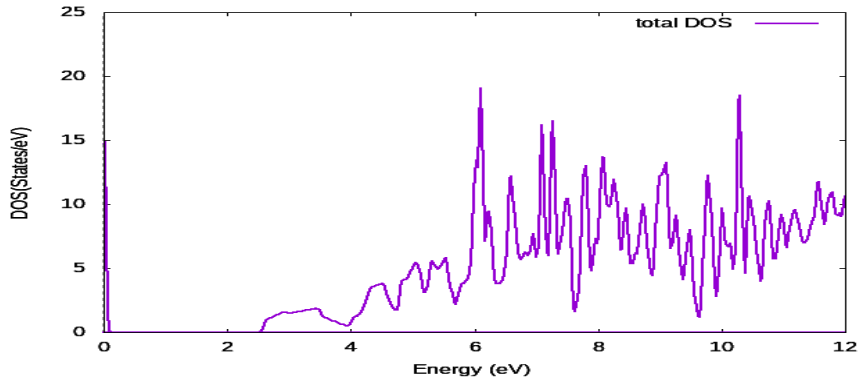

Figure 0.8 : Calculated total density of states (DOS) of KX(X = S)

Density of state KX (X = Te)

An electronic attribute is the spin polarized density of states. The thicknesses of conditions can be utilized to dive further into band structure (DOS). It has been concluded the collective and severed densities of conditions for the KX (X = Te) compound in the CsCl (B2) stage. The unit used for the energy is eV and for the DoS is (states/eV), the emphasis is taken along the x-axis and DoS is on the y-axis. The PDOS of the outermost layers of orbital elements (f of KX & p of X) for the compounds KX (X = S & TE) and KX (X = S & Te) are respectively. The p-valence electrons of X (X = S & Te) contribute mostly to the electronic structure. An atom-projected in the broad PDOS spectrum with a strong peak dominating the region around the Fermi level and a small contribution from the 5f-KX states (EF).

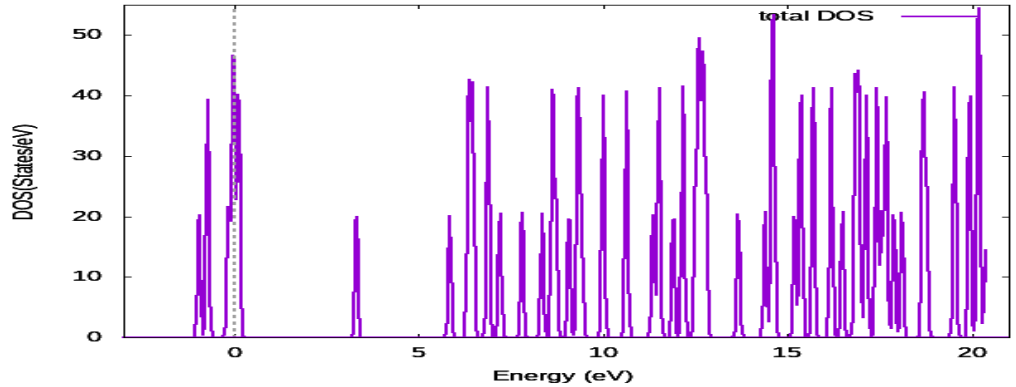

Figure 0.9 : Calculated total density of states (DOS) of KX (X = Te)

Optical properties

Optical properties of KX (X = S)

There are many issues in measuring the optical characteristics of solids. To comprehend how materials behave, it is necessary to compute the dielectric function, which is a crucial quantity.[11] There is only one component calculated for the cubic system. Energy eigen values and electronic wave patterns are taken into account while calculating dielectric functions. These are the organic results of calculations on ab initio band structures, which are often done using a local density approximation (LDA). [12]

Annual Methodological Archive Research Review
http://amresearchreview.com/index.php/Journal/about
Volume 3, Issue 9 (2025)

Online ISSN 3007-3197
Print ISSN 3007-3189
http://amresearchreview.com/index.php/Journal/about

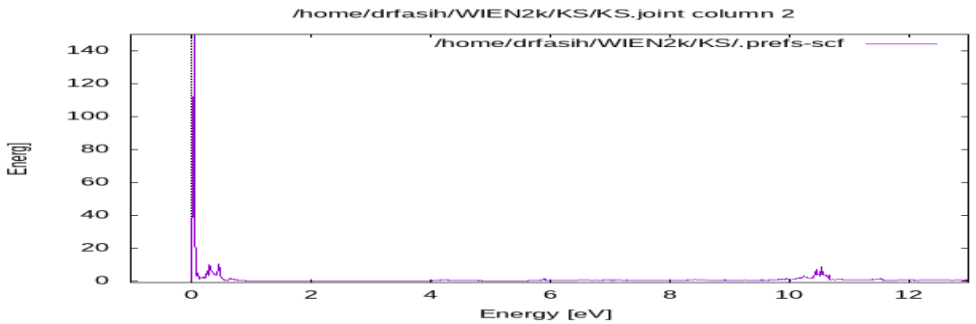

Figure 0.10 : Optical property plot of KX (X = S)

Optical Properties of KX (X = Te)

Using a standard expression, the dielectric function is calculated. Based on the theory given in the previous part, the LMTO-ASA method has been used to compute the optical conductivity and dielectric function. Within LMTO - ASA, optical parameters are all first explicitly determined before being computed. Calculate the Brillouin Total Zone's KXX = (KX (X = S & TE) and KX (X = S & Te) K-scores (BZ). The calculation's outcomes are as follows. Graphical representations of optical conductivity and total hypothetical dielectric function are provided.

Conclusions

In current research, binary alkali-metal chalcogenides are examined by means of density functional theory. In which the linearized augmented plane-wave approach is used on the basis of first principal calculations. The exchange-correlation energy and potential of several substances in various crystalline phases were measured using GGA-PBE and mBJ-GGA-PBE. The KX binary compounds are stable in the nonmagnetic phase. Electronic band structure and density of states of spin-polarized P orbital's in group VI elements indicate half-metallic and magnetic characteristics. The KSe and KTe in the various phases" show HM character in all phases as portrayed. These properties are not common in S and Te based alkali-metal compounds. The bandgaps and optical absorption intensities of these two materials, "KS" and "KTe," make them ideal for photovoltaics and infrared sensing applications. It has been determined that S and Te have a majority-spin carrier band structure and density of states, respectively. The finding of 1.29 eV direct bandgap for KS, a 1.47 eV direct bandgap, and a 0.98 eV indirect bandgap for KTe The chromium d orbitals and the chalcogenide p orbitals are principally responsible for driving the density of states near the conduction band and valence band borders in both structures. Finally, the density of states for KS and KTe conduction band is extraordinarily high.

References

Moradi, M., Rostami, M., & Afshari, M., "Half-metallic ferromagnetism in Wurtzite M S (M = Li, Na, K)", Canadian Journal of Physics, 90(6):531-536 (2012).

Abbouni, N. et al., "Ab-Initio Prediction of Intrinsic Half-Metallicity in Binary Alkali-Metal Chalcogenides: K X (X = S, Se and Te)", International Journal of Materials, Manufacturing and Machinery, (2018) (via World Scientific).

Bouroushian, M., Electrochemistry of Metal Chalcogenides, Springer (2010) - general

Online ISSN 3007-3197
Print ISSN 3007-3189

reference on chalcogenides.

Ali, B., & Abbad, A. (2016). Structural, half-metallic magnetism and elastic properties of the $KMnQ_2$ (Q = O, S, Se, Te) chalcogenides from first-principles calculations. Journal of Magnetism and Magnetic Materials, 401, 145-154.

Abbas, S. M., et al. (2019). First-principles study of structural and electronic properties of alkali-metal chalcogenides: M_2X (M: Li, Na, K, Rb; X: O, S, Se, Te). arXiv preprint arXiv:1903.08112.

Alay-e-Abbas, S. M., & Shaukat, A. (2011). First-principles study of structural and electronic properties of alkali metal chalcogenides: KX (X = S, Se and Te). International Journal of Modern Physics B, 25(12), 3911–3920.

Zhuravlev, Y. N. (2022). Ab initio studies of the influence of pressure on the structure and electronic and elastic properties of alkaline and alkaline-earth metal carbonates [Article]. Computational Materials Science, [Volume], [Pages]. (Note: parameters of the Birch–Murnaghan equation of state are discussed.)

Ain, A., Ong, S. P., Hautier, G., Chen, W., Richards, W. D., Dacek, S., Cholia, S., Gunter, D., Skinner, D., Ceder, G., & Persson, K. A. (2011). Formation enthalpies by mixing GGA and GGA + U calculations. Physical Review B, 84(4), 045115.

Abbouni, N., Zerarga, F., & Bouhemadou, A. (2018). Ab-initio prediction of intrinsic half-metallicity in binary alkali–metal chalcogenides: KX (X = S, Se, Te). International Journal of Materials, Manufacturing and Machinery, (Special Issue), 1-12.

Syrotyuk, S. V., & Shved, V. M. (2015). Quasiparticle electronic band structure of the alkali metal chalcogenides M_2A (M: Li, Na, K, Rb; A: O, S, Se, Te). Condensed Matter Physics, 18(3), 33702-1–8.

Han, Z., Lee, C., Song, J., Wang, H., Bermel, P., & Ruan, X. (2023). Temperature-dependent full-spectrum dielectric function of semiconductors from first principles. Physical Review B, 107(20), L201202.

Marinopoulos, A. G. (2024). Dielectric response of yttria–zirconia ordered solids within density-functional theory in the random-phase approximation. Condensed Matter, 9(4), 54.